Magneto-optical trap operating on a magnetically induced level-mixing effect

K. Nasyrov,[1,*] V. Biancalana,[1] A. Burchianti,[1] R. Calabrese,[2] C. Marinelli,[1] E. Mariotti,[1] and L. Moi[1]
[1]*INFM-UdR di Siena and Dipartimento di Fisica, Università di Siena, Via Banchi di Sotto 55, 53100 Siena, Italy*
[2]*Dipartimento di Fisica, Università di Ferrara and INFN–Sezione di Ferrara, Via Paradiso 12, 44100 Ferrara, Italy*
(Received 15 November 2000; published 6 July 2001)

In this work we point out a theoretical picture accounting for some unpredicted trapping conditions that have been observed—but not satisfactorily explained—in the past and have been recently confirmed by our experiments. We have realized a sodium magneto-optical trap working on the $3\,^2S_{1/2}(F=1)\rightarrow 3\,^2P_{3/2}(F'=0)$ transition that, according to the usually accepted model, should not work. Our results, with respect to the previous unexplained observations, support more stringent conclusions because our experimental setup gives us the possibility to repump atoms from the $F=2$ state using D_1 transitions. This definitely excludes that the repumping frequency may play a role in the trap dynamics. A peculiar perturbation approach allows us to demonstrate that the confinement force originates, in this case, from a magnetically induced level-mixing effect. Moreover, we describe separately the nature of damping and confining forces and we recognize that in this case they are due to different transitions. Trap simulations based on a dynamical three-dimensional model are presented, which quantitatively reproduce our experimental results.

DOI: 10.1103/PhysRevA.64.023412 PACS number(s): 32.80.Pj, 42.50.Vk, 32.60.+i

I. INTRODUCTION

Magneto-optical traps (MOT's) allow for efficient cooling and trapping of neutral atoms. They have been in worldwide use since the 1980s [1], giving spectacular results, by products and applications [2]. But we want to stress that even extensively checked systems (see, e.g., [1,3–5]), as for example the sodium magneto-optical traps, may deserve further investigation as a consequence of interesting and unexplained features.

The MOT efficiency is determined by the cooling rate and by the strength of the atomic confinement in the trap region. Usually three pairs of red detuned and equally intense counterpropagating laser beams are used to slow down the atoms. Thanks to the Doppler effect, moving atoms absorb more photons from the counterpropagating beam than from the copropagating one. Because of that, a slowing force—due to the recoil effect—arises. Actually, this is the basic mechanism of the so-called ''optical molasses'' [5]. In optical molasses atoms are slowed in the whole volume enlightened by the laser beams but they are not confined or collected in a given region.

Using the spatially inhomogeneous magnetic field solves this latter problem. The magnetic field shifts the Zeeman sublevels that depend on the magnetic quantum number M and in the configuration of two counterpropagating beams, with $\sigma=+1$ and $\sigma=-1$ polarization, a position-dependent net force arises. Since a magnetic field gradient exists along all the three beam axes, the position-dependent net force is toward the center, provided that the sign of the magnetic field gradient is suitably set, with respect to the polarization of the beams. In this sense the Zeeman effect produces the confinement force required to make the trap stable.

The qualitative pictures of the arising slowing and confinement forces are presented in Figs. 1(a) and 1(b), respectively, for an ideal $J=0\rightarrow J'=1$ two-level atom. Both the slowing force (due to the Doppler effect) and the confining force (due in this case only to the Zeeman shift of the magnetic sublevels) result from the interaction of red-detuned and circularly polarized light radiation with a given optical atomic transition.

However, in the presence of a closely spaced multilevel scheme (as in the hyperfine structure of the $P_{3/2}$ state of the Li, Na, and K alkali metals), the situation may significantly change. The effective slowing force may be produced in this case by the interaction of light with one or more atomic transitions, whereas the confining force may originate from one of these same transitions, or even from another one. If this is the case, it may happen that the two forces do not work properly and the trapping condition is not achieved.

A detailed analysis of the level structure involved in both the cooling and confining forces is then needed in order to evaluate the trapping efficiency. In particular, the role of the Zeeman pumping has to be carefully reconsidered. In fact, in the usual theoretical interpretation, Zeeman pumping prevents trapping with transitions having the total angular momentum smaller in the excited level than in the ground level.

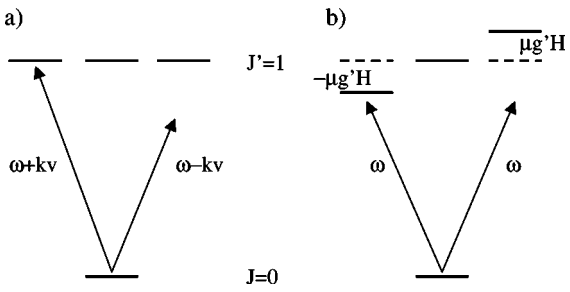

FIG. 1. Resonance conditions responsible for the slowing force due to the Doppler effect (a) and of the confining force due to the Zeeman level shift (b) in a $J=0\rightarrow J=1$ transition. kv and $\mu g'H$ are the Doppler shift and the Zeeman shift, respectively.

*Permanent address: Institute for Automation and Electrometry, Novosibirsk 630090, Russia.

The traditional MOT scheme works in fact for any $J_g \rightarrow J_e = J_g + 1$ transition: atoms scattering mainly from the $\sigma = +1$ laser beam will be optically pumped toward the $M_g = +J_g$ substate, which forms a closed system with the $M_e = +J_e$ substate. On the contrary, a worse trapping condition or even no trapping at all should be obtained for a $J_g \rightarrow J_e = J_g - 1$ transition and in particular for the $3^2S_{1/2}(F=1) \rightarrow 3^2P_{3/2}(F'=0)$ sodium transition (in this case, due to the hyperfine structure, F is the actual total angular momentum to be considered). In fact, as will be thoroughly discussed in the following, in the steady-state condition the Zeeman sublevel populations of the ground state get values, making the number of absorbed photons from the respective sublevel equal to the number of atoms decaying from the excited state to that specific sublevel. As a consequence no radiation force will arise unless an asymmetry in the decay to the ground-state Zeeman sublevels exists.

On the contrary, we show and discuss in the following a trap working on the $F=1 \rightarrow F'=0$ transition. This same trap was observed a few years ago by Shang *et al.* [6]. They related the observation to the $F=1 \rightarrow F'=1$ transition because they observed it even on the blue wing of the $F=1 \rightarrow F'=0$ line profile. In this paper we give a completely different interpretation and we demonstrate that no confinement force is produced by the $F=1 \rightarrow F'=1$ transition, while a confinement force can be obtained even on the blue side of the $F=1 \rightarrow F'=0$ transition. The origin of this force is in a peculiar level-mixing effect induced by the magnetic field.

In our theoretical description of the MOT dynamics, we analyze independently the damping force, that is necessary to slow down the atoms, and the spring force which confines them in the zero-field trap center. Such an analysis is not uncommon in literature, but we use it to show in an easier way the peculiarity of a multiple-line contribution to the damping force. At the same time, the distinction between the two forces allows us to introduce the theoretical scheme where the confining force produced by the level-mixing effect is fully explained.

II. THEORY

The theory of the mechanism that produces the confinement force for the $F=1 \rightarrow F'=0$ optical transition in the sodium D_2 line is presented here. This theory can be extended to other atomic species with a similar level scheme. The calculation reported in this section extracts the most relevant features of the involved phenomena, allowing for a direct physical understanding. They are performed on the basis of the perturbation theory, even if such an approximation is not strictly necessary. Indeed, a numerical approach can be also profitably used, and actually a more precise, numerical computation is considered in the following where the experimental results are discussed and compared to the theoretical predictions.

We first discuss the main features of the force arising in the traditional scheme, which is induced by the Zeeman shift of the level. The force induced by the mixing effect is then described, and it is shown that it accounts for the observation of the unexpected $F=1 \rightarrow F'=0$ trap. In the following, the presence of a second laser frequency (repumping radiation) is considered and its contribution to the force is analyzed. Finally, the effects of the hyperfine structure of the sodium excited states is considered and a peculiar multi line cooling process is discussed.

A. The confining force in the case of the "traditional" scheme: F_{Zeeman}

Let us first reiterate how the confinement force arises in the traditional scheme [1]. For simplicity we consider a two-level atom with a $J=0 \rightarrow J'=1$ optical transition interacting with two counterpropagating waves having equal intensities and opposite circular polarization, respectively [see Fig. 1(b)]. We restrict our analysis to the weak light intensity case, so that the excited state $J'=1$ can be assumed to be much less populated than the ground state $J=0$. The number of photons absorbed per unit time by a slowed atom from the two waves having opposite circular polarization is

$$R_\sigma = \frac{\Gamma G^2}{(\Gamma/2)^2 + (\Omega - \sigma \mu g' H/\hbar)^2}, \tag{1}$$

where the index σ (with the values $\sigma = \pm 1$) refers to the two polarization components; Ω is the frequency detuning of laser radiation with respect to the center of the optical transition; Γ is the rate of the spontaneous decay of the excited state; $G = Ed/\hbar$ is the Rabi frequency, i.e., the cycling rate between the two levels; μ is the Bohr magneton; g' is the Landé factor of the excited state; and H is the amplitude of the magnetic field. As the absorbed photons are isotropically emitted by spontaneous emission, the recoil due to the absorption produces an average $\hbar k R_\sigma$ slowing force acting on the atoms along the direction of propagation of the wave. If the magnetic field is nonzero, the unbalanced force acting on slowed atoms due to counterpropagating waves is

$$\begin{aligned} F_{Zeeman} &= \hbar k (R_{+1} - R_{-1}) \\ &= \hbar k \Gamma G^2 \left[\frac{1}{(\Gamma/2)^2 + (\Omega - \mu g' H/\hbar)^2} \right. \\ &\quad \left. - \frac{1}{(\Gamma/2)^2 + (\Omega + \mu g' H/\hbar)^2} \right]. \end{aligned} \tag{2}$$

In the three-dimensional case, such a force is present in any point along all the directions with the exception of the trap center, where both H and F_{Zeeman} are equal to zero.

Let us consider for simplicity one arbitrary beam direction and let us refer to it as the z axis. This is not a real restriction to a one-dimensional (1D) model and the formalism can be easily extended to the three-dimensional (3D) case.

The z component of the quadrupole magnetic field produced by a pair of anti-Helmholtz coils for small values of z, i.e., close to the trap center can be represented in the form $H_z(z) = H'z$, where $H' = \partial H_z / \partial z|_{z=0}$ is the gradient of the magnetic field in the trap center. Therefore, as soon as the atom moves away from the trap center, it is affected by a

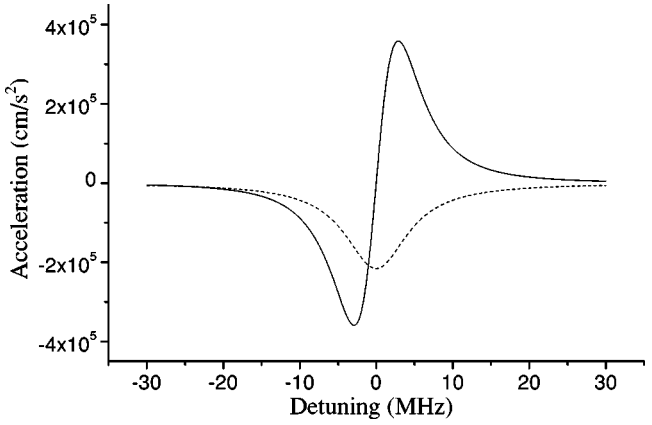

FIG. 2. The acceleration induced on Na atoms by F_{Zeeman} as expressed in Eq. (3) is plotted by the solid curve. The dashed curve allows a direct comparison with the acceleration induced F_{mixing} as calculated using Eq. (15). Both forces are evaluated for $G=1$ MHz and $H=1$ Gauss.

nonzero magnetic field and it undergoes the force (2), which for small z is approximated by

$$F_{Zeeman}=\frac{4kG^2\Gamma\Omega}{[(\Gamma/2)^2+\Omega^2]^2}\mu g' H' z. \tag{3}$$

For red detuning ($\Omega<0$) and positive magnetic field gradient ($H'>0$) this force works as a confining force. It is important to note some relevant features of this force as a function of the detuning: F_{Zeeman} vanishes at exact resonance; it changes its sign depending on the detuning sign; it achieves its maximum absolute value at $|\Omega|=\Gamma/(2\sqrt{3})$; it decreases as Ω^{-3} at large detunings. These features are sketched in the plot represented in Fig. 2, where the solid line is the plot of the acceleration of Na atoms subjected to the force (3) as a function of the detuning; the meaning of the dashed plot is explained in the Sec. II B.

B. The confining force working in the case of the $F=1\rightarrow F'=0$ transition: F_{mixing}

Let us now consider how the confining force arises using radiation in resonance with the $F=1\rightarrow F'=0$ transition of the D_2 line in Na. The structure of the hyperfine levels of the ground $S_{1/2}$ and excited $P_{1/2}$, $P_{3/2}$ states for sodium is sketched in Fig. 3, reporting the most relevant parameters. It is important to point out that, if we neglect the presence of other hyperfine levels and we consider a two-level atom only involving the $F=1\rightarrow F'=0$ transition, we do not get any confining force. In fact, due to optical pumping into the $M=0$ Zeeman sublevel of the ground state, this system would no longer interact with the two circularly polarized waves. Actually, such a 1D analysis is not suitable for a good description of the MOT, as the other orthogonal laser beams prevent such an optical pumping to the $M=0$ sublevel. Nevertheless, even if such an optical pumping to the $F=1$, $M=0$ is prevented, the $F=1\rightarrow F'=0$ transition would not be a driving system, because the excited state has equal probabilities to decay into the $M=-1$ and $M=+1$ levels of the ground state [7,8]. Therefore, in the steady-state regime, atoms should absorb equal numbers of photons from the $\sigma=+1$ and $\sigma=-1$ polarized waves, respectively. As a consequence, the total force coming from each couple of counterpropagating waves would vanish, independently of their detunings and intensities. Actually, as described in [8], a peculiar cooling effect may originate in Λ systems, due to atom diffusion in the impulse space, which brings atoms in a *dark state*, where they are stored at very low temperature. Nevertheless such a mechanism is not related to a regular force, which actively slows down the atoms, and it cannot be considered a driving system for the MOT.

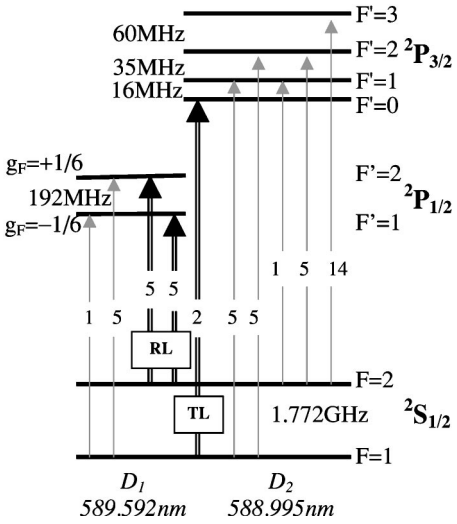

FIG. 3. The $3S$ and $3P$ level structure of sodium with a sketch of the laser-induced transitions used in the experiment. RL is the repumping laser; TL is the trapping laser. The energy separation between the levels is expressed in frequency units.

In spite of these strict theoretical considerations, traps operating with sodium in the $F=1\rightarrow F'=0$ have been experimentally observed both by us and by Shang *et al.* [6]. Here we show that different phenomena need to be taken into account, for a correct interpretation of these observations.

First of all, the two-level model considered above is not valid in the case of sodium as well as of some other alkali metals because the hyperfine levels of the excited state $P_{3/2}$ are closely spaced with each other and even moderate magnetic fields can induce considerable mixing among them. We show that this mixing destroys the symmetry of spontaneous decay from the excited state to the Zeeman sublevels of the ground state, allowing for the inset of an unbalance in the absorption of $\sigma=+1$ and $\sigma=-1$ photons. Moreover, it is very important to remark that this unbalance is only related to the sign of the magnetic field, so that no red detuning is needed for producing the confining force by means of this mechanism.

We want also to stress that this force may only act on confining atoms whose velocity has been already slowed down. In fact, such a force cannot be used for the slowing process, because it does not depend on the atom velocity. This statement points out an important difference from the Zeeman force. In fact it comes out from the scheme in Fig. 1 that the Zeeman force confines the slowed atoms, but it also

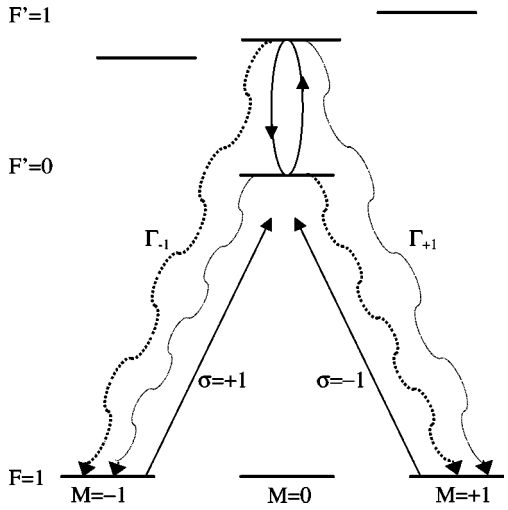

FIG. 4. Sketch of the double three-level Λ system considered in the model. The two straight arrows represent the laser excitation; the broken arrows give the decay by spontaneous emission; the circle represents the mixing between the two $M=0$ levels of the excited states. The $\Gamma_{\pm 1}$ are the decay rates, whose differences are represented in terms of the thickness of the broken arrows.

provides a damping effect slowing down their velocity.

The nature of the $F'=0$ decay symmetry breaking has an analogy with an alignment-orientation conversion phenomenon. This latter was already known and studied for alkali-metal atoms (see, e.g., [9] and [10]). The origin of these phenomena lays on a joint action of the magnetic field and of the hyperfine interaction.

Let us consider a three-level atom model (Fig. 4) having one ground state $F=1$ and two slightly separated excited levels $F'=0$ and $F'=1$ (we neglect for simplicity the $F'=2$ and $F'=3$ levels). In the system of coordinates with the z axis directed along the magnetic field, the operator of the electron interaction with the magnetic field is

$$\hat{V}=\mu g' H \hat{J}_z, \tag{4}$$

where $\hat{J}_z$ is the operator of the z component of the total electron angular momentum. Let us consider the case of weak magnetic field, so that the potential is much smaller than the zero-field energy splitting ΔE between the $F'=0$ and $F'=1$ states and the ordinary perturbation theory can be applied. Otherwise, the secular equation should be solved, as in the Paschen-Back approach. Moreover, we will neglect the terms of H^2 order and, in particular, the energy shift of the $M'=0$ levels.

Due to the selection rules, the nondiagonal matrix element of the interaction potential is nonzero only for $M'=0$ sublevels of $F'=0$ and $F'=1$ states. In other words, the mixing is possible only between the $M'=0$ sublevels. We introduce the following notation:

$$V_{10}=\langle F'=1,\, M'=0|\hat{V}|F'=0,\, M'=0\rangle, \quad V_{01}=V_{10}^* \tag{5}$$

for nondiagonal matrix elements of the interaction potential, where $|F,M\rangle$ are eigenfunctions of the total angular momentum. On the basis of the perturbation theory the stationary states result

$$|F'=1,\, M'=0\rangle_H=|F'=1,\, M'=0\rangle+\frac{V_{10}}{\Delta E}|F'=0,\, M'=0\rangle, \tag{6}$$

$$|F'=0,\, M'=0\rangle_H=|F'=0,\, M'=0\rangle-\frac{V_{01}}{\Delta E}|F'=1,\, M'=0\rangle,$$

where the index H denotes that these are the new stationary states for the nonzero magnetic field.

Using these new wave functions we derive the matrix elements of the dipole moment for the transitions connecting excited states to ground states: ${}_H\langle F',M'|d_\sigma|F,M\rangle$, where d_σ is a circular component of the dipole vector. As a consequence of Eq. (6), the d_σ matrix elements are

$$\begin{aligned} {}_H\langle F'=0,\, M'=0|d_\sigma|F=1,\, M\rangle &= \langle F'=0,\, M'=0|d_\sigma|F=1,\, M\rangle \\ &\quad -\frac{V_{10}}{\Delta E}\langle F'=1,\, M'=0|d_\sigma|F=1,\, M\rangle, \end{aligned} \tag{7}$$

$$\begin{aligned} {}_H\langle F'=1,\, M'=0|d_\sigma|F=1,\, M\rangle &= \langle F'=1,\, M'=0|d_\sigma|F=1,\, M\rangle \\ &\quad +\frac{V_{01}}{\Delta E}\langle F'=0,\, M'=0|d_\sigma|F=1,\, M\rangle, \end{aligned}$$

where, according to the selection rules, the matrix elements are nonzero only if $M=-\sigma$.

It is important to remark here that, due to the properties of the Clebsh-Gordan coefficients, the $\langle F'=0,\, M'=0|d_\sigma|F=1,\, M=-\sigma\rangle$ matrix elements are symmetric and the $\langle F'=1,\, M'=0|d_\sigma|F=1,\, M=-\sigma\rangle$ ones are antisymmetric with respect to the $\sigma\rightarrow-\sigma$ replacement. Therefore, the matrix elements (7), due to $F'=1\leftrightarrow F'=0$ level mixing, become asymmetric for nonzero magnetic field. Since the spontaneous decay of the excited state $F',M'=0$ into ground state F,M is

$$\Gamma_M=\Gamma(F',M'=0\rightarrow F,M)\propto\left|{}_H\langle F',M'=0|d_{-M}|F,M\rangle\right|^2, \tag{8}$$

this asymmetry induces an asymmetry in the spontaneous decay of the excited states. The direct calculation [11] for the case of the Na $S_{1/2}\rightarrow P_{3/2}$ transition gives

$$\langle F'=0,\ M'=0|d_{-M}|F=1,M\rangle=(-1)^{1-M}\frac{d}{2\sqrt{3}},$$

$$\langle F'=1,\ M'=0|d_{-M}|F=1,M\rangle=-(-1)^{1-M}\frac{\sqrt{5}d}{4\sqrt{3}}M, \tag{9}$$

$$V_{10}=V_{01}=\frac{\sqrt{5}}{2}\mu g' H,$$

where d is the reduced matrix element of the dipole moment for the transition $S_{1/2}\rightarrow P_{3/2}$. Using Eqs. (7)–(9) the spontaneous decay rate of the state $F'=0, M'=0$ into states $F=1,M$ results in

$$\Gamma_M=\frac{\Gamma}{3}\left(1+\frac{5}{4}\frac{\mu g' H}{\Delta E}M\right)^2. \tag{10}$$

Now we can evaluate the confining force as it arises for the $F=1\rightarrow F'=0$ transition. For simplicity, instead of the quantum system shown in Fig. 4, we consider a three-level Λ system, by ignoring the Zeeman sublevel $|F=1,\ M=0\rangle$ of the ground state. This is allowed, because the optical pumping in that level is prevented by the orthogonal laser beams, which actually exist in the MOT even if they do not contribute directly to establish the force in the z direction.

For such a Λ system one can obtain the equation for motion (see Appendix)

$$\frac{\partial}{\partial t}\rho+\frac{p}{m}\frac{\partial}{\partial z}\rho+(\Gamma_{-1}-\Gamma_{+1})\hbar k\frac{\partial}{\partial p}\rho_{00}=0. \tag{11}$$

Here ρ is the atom density and ρ_{00} is the density of atoms in the excited state. The last term in Eq. (11) describes the dynamics of an atom due to radiation force, which is clearly vanishing for $\Gamma_{-1}=\Gamma_{+1}$, as first stated in [7]. Such a radiation force is proportional to the population of atoms in the excited state. If we indicate by $s=\rho_{00}/\rho$ the fraction of atoms in the excited state, the force value results

$$F=\hbar k(\Gamma_{-1}-\Gamma_{+1})s. \tag{12}$$

This equation clearly shows that such a confining force originates from the asymmetry in the spontaneous decay of the excited state $F'=0$, which in turn is due to the mixing induced by the magnetic field.

To obtain the explicit expression for the value of s we can use the results of [12] and [13]. Applying these results for our case we find

$$s=\frac{G^2}{\left(\frac{\Gamma}{2}\right)^2+\Omega^2+G^2+\omega_H^2+\frac{G^4}{\omega_H^2}+\frac{\Gamma_{-1}-\Gamma_{+1}}{\Gamma}\left(2\omega_H-\frac{G^2}{\omega_H}\right)\times\Omega}, \tag{13}$$

where G and Ω are Rabi frequency and detuning, respectively, $\omega_H=\mu g H$ is the Larmor frequency, and g is the Landé factor for the ground state. If we consider the case of low radiation intensity and any atom displacement from the trap center so that

$$\omega_H\sqrt{\left(\frac{\Gamma}{2}\right)^2+\Omega^2}\gg G^2 \tag{14}$$

and take into account only the terms that are linear with respect to H, from Eqs. (10), (12), and (13) we obtain

$$F_{mixing}=-\hbar k\frac{5}{3}\frac{\mu g' H}{\Delta E}\frac{\Gamma G^2}{(\Gamma/2)^2+\Omega^2}, \tag{15}$$

while in the other limit, opposite to Eq. (14), we would get for the confining force

$$F_{mixing}=-\hbar k\frac{5}{3}\frac{\mu g' H}{\Delta E}\frac{(\mu g H)^2}{G^2}. \tag{16}$$

This latter quantity is proportional to z^3 and hence such a force can work only in a small region very close to the trap center. In this paper we consider conditions when force [Eq. (15)] can be applied.

The acceleration induced on sodium atoms by this force is represented in the dashed plot of Fig. 2. The plot, as well as the analysis of Eq. (15), clearly shows the differences between the mixing force and the Zeeman force, expressed in Eq. (3). F_{mixing} does not change its sign with the detuning sign; it achieves its maximum value at zero detuning and decreases as Ω^{-2} for large detunings. It is interesting to make a comparison between Eqs. (3) and (15) calculated at the detunings corresponding to the maxima of the two forces. The two detunings are $|\Omega|=\Gamma/(2\sqrt{3})$ for F_{zeeman} and $|\Omega|=0$ for F_{mixing}, respectively. The result shows that the typical relative intensities of F_{Zeeman} and F_{mixing} forces are related according to

$$F_{mixing}\approx\frac{\hbar\Gamma}{\Delta E}F_{Zeeman}.$$

A sodium atom in the $P_{3/2}$ state has $\Gamma=10$ MHz and $\Delta E/\hbar=16$ MHz, so that the two forces have the same order of magnitude. The two forces have the same sign for red detuning ($\Omega<0$), while the Zeeman force changes it sign for blue detuning.

It turns out from Eq. (7) that the asymmetry of spontaneous decay of the $M'=0$, $F'=1$ excited level is opposite the one of the $M'=0$, $F'=0$ state. Therefore, the force coming from the $F=1\rightarrow F'=1$ transition has the opposite sign with respect to the force coming from the $F=1\rightarrow F'=0$ transition. It follows that if the polarization of the counterpropagating waves and the sign of the magnetic field gradient are set in such a way to make the $F=1\rightarrow F'=0$ transition responsible for a confining force, then the $F=1\rightarrow F'=1$ transition produces a repelling force.

Therefore, with such a choice of polarization and magnetic field gradient, the total force produced by the two transitions confines the atoms for detuning near resonance with a $F=1\rightarrow F'=0$ transition, it vanishes at some intermediate

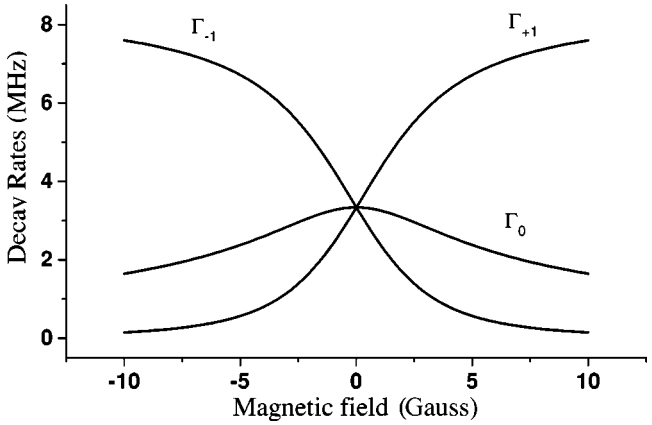

FIG. 5. The spontaneous decay rates of the $F'=0$ state to the Zeeman sublevels $M=-1$ (Γ_{-1}), $M=0$ (Γ_0), and $M=1$ (Γ_{+1}) of the $F=1$ state.

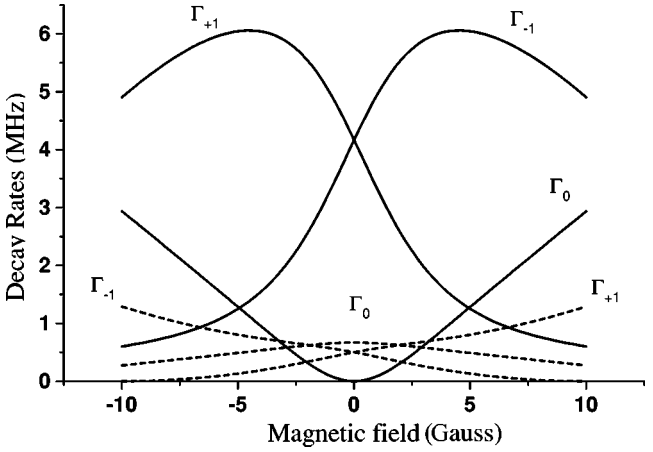

FIG. 6. Spontaneous decay rates of the $F'=1$, $M'=0$ state to the $M=-1$ (Γ_{-1}), $M=0$ (Γ_0), and $M=1$ (Γ_{+1}) Zeeman sublevels of the $F=1$ state (solid lines) and of the $F=2$ state (dashed lines) as a function of the magnetic field intensity.

frequency, and eventually it repels atoms when the frequency is set closer to the resonance with an $F=1\rightarrow F'=1$ transition.

In reality, the picture is even more complicated because of the other $F'=2,3$ levels of the hyperfine manifold of the $P_{3/2}$ state of Na. For instance, the $F=1\rightarrow F'=2$ transition gives a confining force with the same signs as the $F=1\rightarrow F'=0$ transition. Anyway, due to the larger energy separation of the $F'=2$, 3 states, they produce only slight corrections on the final value of F_{mixing}.

C. Role of the repumping frequency in the trap dynamics

This analysis must be completed by taking into account the level structure of the ground state and the decay rate of the atoms from the $F'=1$, 2, 3 excited levels to the $F=2$ level of the ground state. An additional frequency—the repumping frequency—is in fact needed to prevent the optical pumping of the $F=2$ ground-state level, and the contributions to the force arising from this latter radiation may be relevant. Such an analysis of the trapping dynamics has already been experimentally performed and theoretically studied using a numerical model for a 3D sodium MOT [14]. The model is indeed applicable also to the other alkali-metal atoms. It takes into consideration all the possible transitions between states $S_{1/2}$, $P_{1/2}$, and $P_{3/2}$ as well as the level mixing due to magnetic field.

This numerical model has been applied also to the analysis of the $F=1\rightarrow F'=0$ trap. In Fig. 5 the decay rates of the $F'=0$ level into the $M=0,\pm 1$, $F=1$ states as a function of the magnetic field magnitude are shown, while in Fig. 6 the decay rates are plotted of the $F'=1$, $M'=0$ state to the $F=1$ and $F=2$ states. A direct comparison of Figs. 5 and 6 shows the opposite sign of the H field effect on the spontaneous decay rates of $F'=0$, $M=0$ and $F'=1$, $M=0$ to the $F=1$, $M=\pm 1$ ground states.

The acceleration produced by the confining forces, calculated for the different transitions, and the net acceleration are reported in Fig. 7 as a function of the frequency detuning of the laser. The laser is on resonance with the D_2 line and the accelerations are calculated for a 1 Gauss magnetic field. This is a typical value in our experiment, where $H'\cong 10$ Gauss/cm, and the trap size is of the order of $2-3$ mm. The repumping laser is assumed to be in resonance with the $F=2\rightarrow F'=2$ transition of the D_1 line (see Fig. 3). The negative values of the acceleration correspond to confining forces, and positive values correspond to repelling forces. Figure 7 shows that two of the forces coming from the $F=1\rightarrow F'=0$, transitions are confining forces, while the force coming from the $F=1\rightarrow F'=1$ transition is repelling.

The largest acceleration is mainly due to the $F=1\rightarrow F'=0$ transition and it is in the $\Omega<-100$ MHz detuning region (we have set the $\Omega=0$ detuning to correspond to the energy separation between the two states $F=1$ and $F'=3$). There is another region that corresponds to the -80 MHz $<\Omega<-60$ MHz detuning, where a confining force exists; but the trap for that detuning range is not efficient because the resulting capture velocity is not large enough.

It is important to stress that, as already stated in [14], the repumping laser may play an important role in determining the force, and in some cases also its detuning is a crucial

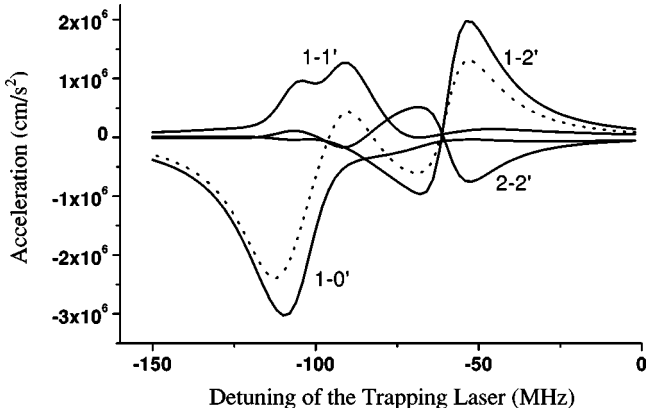

FIG. 7. Total confining acceleration (dashed line) and accelerations due to the forces coming from the different transitions. The values are calculated for 1 Gauss H field. The zero detuning is set at the frequency corresponding the $F=1\leftrightarrow F'=3$ energy separation.

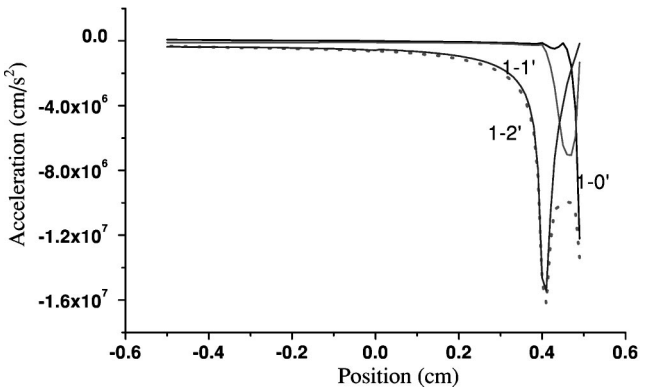

FIG. 8. Total acceleration slowing down the atomic velocity (dashed line) and partial contributions coming from the different transitions as a function of the position in the trap. The atom enters the trap at $z=0.5$ cm and it is stopped at $z\cong+0.5$ cm. A field gradient equal to $H'=10$ Gauss/cm is considered.

parameter. In our experiment, by tuning the repumping laser to the D_1 transition, we have obtained trapping conditions with the repump frequency tuned both to $F=2\rightarrow{}^2P_{1/2}$, $F'=1$ and to $F=2\rightarrow{}^2P_{1/2}$, $F'=2$ transitions. As the Landé factors of the two hyperfine levels of the ${}^2P_{1/2}$ have opposite sign ($g_{F'=1}=-1/6$, $g_{F'=2}=+1/6$), the repumping laser contribution to the force is alternatively confining or repelling. Thus our experiment definitely demonstrates that the confining force is actually given by the mixing force.

D. The cooling force: a multiple line contribution

As we have already pointed out in the Introduction, it is possible that differences exist between the origin of the slowing and of the confining forces. In particular, when the atom is characterized by close-spaced levels in the hyperfine structures, the slowing force can be determined by one or more atomic transitions. It is also possible that these transitions, even if playing a relevant role in the slowing process, do not contribute at all to the confining force. As we have shown, this latter can be even related to a different mechanism, and in particular to the breaking of spontaneous-emission symmetry induced by level mixing.

A detailed description of the roles played by slowing and confining forces involved in the dynamics of trap loading can be obtained by calculating the forces along atomic trajectories. It is possible to point out how several force components, originating from different mechanisms and different atomic transitions, work during a capture process.

In Fig. 8 we show the acceleration of a single atom entering the trap region at $z=-0.5$ cm and being stopped at $z=0.5$ cm. The laser detuning is $\Omega=-110$ MHz, which corresponds to the maximum confining force produced in the $F=1\rightarrow F'=0$ mixing scheme. This figure demonstrates that during almost the whole path of the atom in the trap region, the main role in slowing down its velocity is played by the force originating from the $F=1\rightarrow{}^2P_{3/2}$, $F'=2$ transition. With respect to this transition the laser is quite red-detuned, so that it gives relevant contribution as long as the atom has a large velocity. Only at the end of this path, when the atom has already lost the main part of its kinetic energy, and the Doppler effect is hence decreased, do the forces coming from the $F=1\rightarrow F'=0$, 1 transitions begin to play an important role.

This peculiar multiple-line cooling force reproduces, thanks to the hyperfine atomic structure, a broadband cooling mechanism which is in some sense quite similar to the one proposed and tested in Refs. [15,16]. In that case a multiple-frequency laser radiation was used whereas a single transition of the atomic or ionic system was involved.

III. EXPERIMENTAL RESULTS AND COMPARISON WITH NUMERICAL SIMULATION

Our MOT operates in a spherical glass cell (diameter about 15 cm) with six optical windows placed along right-angle directions; four extra windows are also available for diagnostics. The cell is connected to an ion pump and to a sodium reservoir that can be heated up to produce a suitable vapor density. The residual background pressure limits the trap lifetime to about $\tau\cong 2$ s.

A pair of coils in the anti-Helmoltz configuration gives the requested quadrupole magnetic field with a field gradient of the order of 10 Gauss/cm. Compensating coils are used to eliminate the spurious magnetic fields.

Two independent Ar^+-pumped ring dye lasers generate the trapping and the repumping frequencies. The availability of two independent laser sources instead of a single laser coupled to an electro-optical modulator (as used by other groups [1]) gives us the possibility of tuning the two frequencies to two different fine-structure levels. This is a relevant feature that allowed us to clearly discriminate the contribution to the force coming from the two frequencies, and—as stated above—to demonstrate that only the D_2, $F=1\rightarrow F'=0$ through the level-mixing effect is actually responsible for the trap stability.

The two laser beams are about 1.2 cm in diameter at the trap level; they are overlapped and split in three parts along three orthogonal axes. Three mirrors reflect back the laser beams in each arm of the trap. Suitable $\lambda/4$ plates provide the proper σ polarization to the six beams crossing in the trap center. The $F=1\rightarrow F'=0$ trap is produced keeping the laser beams with the same circular polarization as for "standard" $F=2\rightarrow F'=3$ traps, and this is in agreement with the theoretical prediction.

Both lasers are actively stabilized to thermostatted optical cavities, allowing for a frequency stability of a few MHz over several minutes. Two sodium reference cells are used to set and monitor the laser frequencies with the saturation spectroscopy technique. Namely, the saturation spectroscopy signals are acquired simultaneously with the trap fluorescence during the frequency scan, so that accurate frequency calibration of the scanned laser is available.

The number of trapped atoms can be estimated by measuring the induced fluorescence. charge-coupled device (CCD) cameras allow us to monitor the cloud shape and size, so that the atomic density can be estimated, as well.

The trapping laser (TL) is on resonance with the D_2 line. Its frequency is scanned across the $F=1\rightarrow F'=0$, 1, 2 tran-

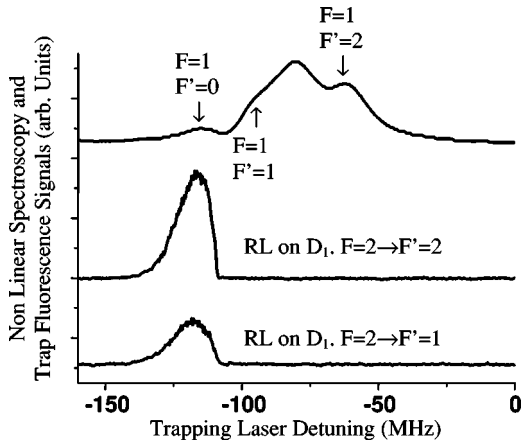

FIG. 9. Experimental signals showing the nonlinear spectroscopy of the trapping laser (curve *a*); the fluorescence intensity of the trap as a function of the trapping laser frequency scanning across the $2S_{1/2}$, $F=1\rightarrow{}^2P_{3/2}$, $F'=0,1,2$ lines when the repumping frequency is tuned to D_1 line, namely to ${}^2S_{1/2}$, $F=1\rightarrow{}^2P_{1/2}$, $F'=1$ (curve *b*) and ${}^2S_{1/2}$, $F=1\rightarrow{}^2P_{1/2}$, $F'=2$ (curve *c*).

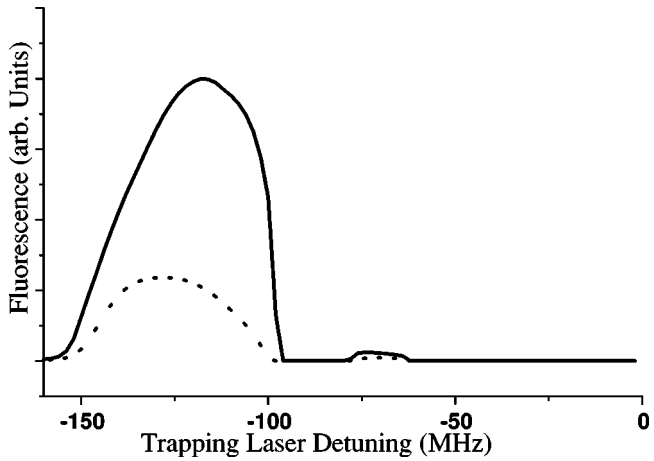

FIG. 10. Calculated trap fluorescence as a function of trapping laser detuning. The repumping laser is in resonance with $F=2\rightarrow F'=2$ (solid line) and $F=2\rightarrow F'=1$ (dotted line) transitions of the D_1 line. A direct comparison with Fig. 9 is possible.

sitions. The repumping laser (RL) is kept on resonance with either the $F=2\rightarrow F'=2$ or the $F=2\rightarrow F'=1$ transitions of the D_1 line. The fluorescence intensity of the trap is measured as a function of the trapping laser detuning and a typical result is shown in Fig. 9 where the saturation spectroscopy signal is also reported, allowing for an absolute calibration of the laser frequency. This figure clearly demonstrates the existence of the trap for the trapping laser frequency corresponding to the $F=1\rightarrow F'=0$ transition. This trap can be observed when the repumping laser frequency is on resonance either with the $F=2\rightarrow F'=2$ transition or with the $F=2\rightarrow F'=1$ one of the D_1line. This definitely demonstrates that the trap confinement is not due to the repumping radiation. In fact, the Landé factors of the $F'=1$ and $F'=2$ levels of the $P_{1/2}$ state have opposite signs, namely $g_{F'=2}>0$, $g_{F'=1}<0$ [17]. Therefore, should the trap confinement be attained thanks to the repumping laser, the trap would exist only for one of the repumping frequencies while it would be unstable for the other one. The fact instead that the trap exists for both repumping frequencies proves that the confining force is effectively due to the D_2 line and it comes from the $F=1\rightarrow F'=0$ transition.

The trap intensities for the two repumping frequencies differ from each other approximately by about a factor 3. The results of the numerical simulation by the trap model described in Ref. [14] are shown in Fig. 10. The frequency position of the trapping region is in perfect agreement with the experimental results, while a slight difference appears in the spectral width of the trap, which is narrower in the experimental results than in the calculation. Moreover, a quantitative agreement is observed in the relative intensities of the two traps obtained by setting the repumping frequency on the $F=2\rightarrow{}^2P_{1/2}$, $F=1$ or on the $F=2\rightarrow{}^2P_{1/2}$, $F=2$.

IV. CONCLUSION

In this paper we presented a trapping mechanism in sodium MOT. Differing from the traditional schemes of confinement where Zeeman shifting of magnetic sublevels is exploited, in our model the mechanism producing the confinement is the result of the spontaneous decay asymmetry of excited states induced by magnetic field level mixing. The experimental evidence of this trapping scheme is realized with the $F=1\rightarrow F'=0$ transition of the D_2 line of sodium. The detailed description of such a trap demanded a clear separation between the damping force and the confining force, because they originate from different transitions. As a further peculiarity, the damping force is determined by a multiple line interaction, involving three hyperfine states of the excited level. This is somehow a complementary scheme to the broad band laser cooling, where multiple line laser radiation is used to cool down atoms or ions tuning the frequency to one given transition, in a way already tested and proposed also by our group.

ACKNOWLEDGMENTS

We would like to acknowledge the technical help of M. Badalassi, S. Bottari, E. Corsi, A. Marchini, A. Pifferi, and C. Stanghini. This work has been partially supported by the Istituto Nazionale di Fisica Nucleare, Ministero per l'Università e la Ricerca Scientifica e Tecnologica, Università di Siena, Istituto Nazionale di Fisica della Materia. We thank Emilie Jennette for her suggestions and improvements.

APPENDIX

We start from the quantum equation for a Wigner function $\rho(p,z)$, depending on particle impulse p and coordinate z:

$$\frac{\partial\rho}{\partial t}+\hat{\Gamma}\rho+\frac{i}{\hbar}e^{i\hbar\hat{w}/2}(H\rho-\rho H)=0, \tag{A1}$$

where H is the Hamiltonian of the system under consideration, $\hat{\Gamma}$ is the relaxation operator, and $\hat{w}$ is the Poisson brackets operator, which acts as

$$\hat{w}AB=\frac{\partial}{\partial z}A\frac{\partial}{\partial p}B-\frac{\partial}{\partial p}A\frac{\partial}{\partial z}B.$$

For a Λ system with an excited state $|0\rangle$ and two ground states $|-1\rangle$ and $|+1\rangle$, the Hamiltonian has the form

$$H=\frac{p^2}{2m}+H_0|0\rangle\langle 0|+H_{-1}|-1\rangle\langle -1|+H_{+1}|+1\rangle\langle +1|+V,$$

where H_0, H_{-1}, and H_{+1} are the energies of corresponding states and V is the potential of the external perturbation.

Let us consider the interaction of a particle with two counterpropagating waves

$$E=E_+e^{ikz}+E_-e^{-ikz},$$

where the wave E_+ induces transition between states $|-1\rangle$ and $|0\rangle$ and the wave E_- induces transition from the $|+1\rangle$ state to the $|0\rangle$ state. In this case only the potential matrix elements $V_{-10}=V_{0-1}^*$ and $V_{+10}=V_{0+1}^*$ are nonzero and

$$V_{+10}\sim e^{ikz},\quad V_{-10}\sim e^{-ikz}.$$

For the matrix elements ρ_{00}, ρ_{-1-1}, and ρ_{+1+1}, describing the populations of levels $|0\rangle$, $|-1\rangle$, and $|+1\rangle$, respectively, from Eq. (A1) we obtain equations

$$\frac{\partial}{\partial t}\rho_{00}+\frac{p}{m}\frac{\partial}{\partial z}\rho_{00}+\Gamma\rho_{00}+\frac{i}{\hbar}e^{-(\hbar k/2)(\partial/\partial p)}\times[V_{0-1}\rho_{-10}-V_{-10}\rho_{0-1}]+\frac{i}{\hbar}e^{(\hbar k/2)(\partial/\partial p)}\times[V_{0+1}\rho_{+10}-V_{+10}\rho_{0+1}]=0, \tag{A2}$$

$$\frac{\partial}{\partial t}\rho_{-1-1}+\frac{p}{m}\frac{\partial}{\partial z}\rho_{-1-1}-\Gamma_{-1}\rho_{00}-\frac{i}{\hbar}e^{(\hbar k/2)(\partial/\partial p)}\times[V_{0-1}\rho_{-10}-V_{-10}\rho_{0-1}]=0, \tag{A3}$$

$$\frac{\partial}{\partial t}\rho_{+1+1}+\frac{p}{m}\frac{\partial}{\partial z}\rho_{+1+1}-\Gamma_{+1}\rho_{00}-\frac{i}{\hbar}e^{-(\hbar k/2)(\partial/\partial p)}[V_{0+1}\rho_{+10}-V_{+10}\rho_{0+1}]=0. \tag{A4}$$

Here Γ_{+1} and Γ_{-1} are rates of spontaneous decay of excited state $|0\rangle$ into the ground states $|+1\rangle$ and $|-1\rangle$, respectively, so that the global decay rate is $\Gamma=\Gamma_{-1}+\Gamma_{+1}$. Summing Eqs. (A2), (A3), and (A4) we obtain an equation for the total density of atoms $\rho=\rho_{00}+\rho_{-1-1}+\rho_{+1+1}$

$$\frac{\partial}{\partial t}\rho+\frac{p}{m}\frac{\partial}{\partial z}\rho+\frac{i}{\hbar}(e^{-(\hbar k/2)(\partial/\partial p)}-e^{(\hbar k/2)(\partial/\partial p)})\times[V_{0-1}\rho_{-10}-V_{-10}\rho_{0-1}-V_{0+1}\rho_{+10}+V_{+10}\rho_{0+1}]=0. \tag{A5}$$

From Eqs. (A3) and (A4) in the steady-state condition it follows

$$V_{0-1}\rho_{-10}-V_{-10}\rho_{0-1}=i\hbar e^{-(\hbar k/2)(\partial/\partial p)}\Gamma_{-1}\rho_{00}, \tag{A6}$$

$$V_{0+1}\rho_{+10}-V_{+10}\rho_{0+1}=i\hbar e^{(\hbar k/2)(\partial/\partial p)}\Gamma_{+1}\rho_{00}. \tag{A7}$$

Using these expressions and keeping only terms of first order in k, from Eq. (A5) can be obtained

$$\frac{\partial}{\partial t}\rho+\frac{p}{m}\frac{\partial}{\partial z}\rho+(\Gamma_{-1}-\Gamma_{+1})\hbar k\frac{\partial}{\partial p}\rho_{00}=0. \tag{A8}$$

[1] E.L. Raab, M. Prentiss, A. Cable, S. Chu, and D.E. Pritchard, Phys. Rev. Lett. **59**, 2631 (1987).

[2] H.J. Metcalf and P. van der Straten, *Laser Cooling and Trapping* (Springer, New York, 1999).

[3] Z.T. Lu, C.J. Bowers, S.J. Freedman, B.K. Fujikawa, J.L. Mortara, S.Q. Shang, K.P. Coulter, and L. Young, Phys. Rev. Lett. **72**, 3791 (1994).

[4] W. Ketterle, B.D. Kendall, M.A. Joffe, A. Martin, and D. Pritchard, Phys. Rev. Lett. **70**, 2253 (1993).

[5] S. Chu, L. Hollberg, J.E. Bjorkholm, A. Cable, and A. Ashkin, Phys. Rev. Lett. **55**, 48 (1985).

[6] S-Q. Shang, Z-T. Lu, and S.J. Freedman, Phys. Rev. A **50**, R4449 (1994).

[7] V.G. Minogin and Yu.V. Rozhdestvensky, Zh. Éksp. Teor. Fiz. **88**, 1950 (1985) [Sov. Phys. JETP **61**, 1156 (1985)].

[8] A. Aspect, E. Arimondo, R. Kaiser, N. Vansteenkiste, and C. Cohen-Tannoudji, J. Opt. Soc. Am. B **6**, 2112 (1989).

[9] W. Baylis, Phys. Lett. **26A**, 414 (1968).

[10] X.L. Han and G.W. Schinn, Phys. Rev. A **43**, 266 (1991).

[11] I.I. Sobel'man, *Introduction to the Theory of Atomic Spectra* (Pergamon Press, Braunschwaig, 1969).

[12] P.L. Kelley, P.J. Harshman, O. Blum, and T.K. Gustafson, J. Opt. Soc. Am. B **11**, 2298 (1994).

[13] A.V. Taichenachev, A.M. Tumaiken, and V.I. Yudin, Zh. Éksp. Teor. Fiz. **72**, 173 (2000) [JETP Lett. **72**, 119 (2000)].

[14] S.N. Atutov, V. Biancalana, A. Burchianti, R. Calabrese, S. Gozzini, V. Guidi, P. Lenisa, C. Marinelli, E. Mariotti, L. Moi, K. Nasyrov, and S. Pod'yachev, Eur. Phys. J. D **13**, 71 (2000).

[15] S. Gozzini, E. Mariotti, C. Gabbanini, A. Lucchesini, C. Marinelli, and L. Moi, Appl. Phys. B: Photophys. Laser Chem. **54**, 428 (1992).

[16] S.N. Atutov, R. Calabrese, R. Grimm, V. Guidi, I. Lauer, P. Lenisa, V. Luger, E. Mariotti, L. Moi, A. Peters, U. Schramm, and M. Stößel, Phys. Rev. Lett. **80**, 2129 (1998).

[17] J. Flemming, A.M. Tuboy, D.M.B.P. Milory, L.G. Marcassa, S.C. Zilio, and V.S. Bagnato, Opt. Commun. **135**, 269 (1997).